



**HAL**  
open science

## Storylines of Sahel precipitation change: roles of the North Atlantic and Euro-Mediterranean temperature.

Paul-Arthur Monerie, Michela Biasutti, Juliette Mignot, Elsa Mohino,  
Benjamin Pohl, Giuseppe Zappa

### ► To cite this version:

Paul-Arthur Monerie, Michela Biasutti, Juliette Mignot, Elsa Mohino, Benjamin Pohl, et al.. Storylines of Sahel precipitation change: roles of the North Atlantic and Euro-Mediterranean temperature.. *Journal of Geophysical Research: Atmospheres*, 2023, 128 (16), pp.e2023JD038712. 10.1029/2023JD038712 . hal-04188242

**HAL Id: hal-04188242**

**<https://u-bourgogne.hal.science/hal-04188242v1>**

Submitted on 29 Aug 2023

**HAL** is a multi-disciplinary open access archive for the deposit and dissemination of scientific research documents, whether they are published or not. The documents may come from teaching and research institutions in France or abroad, or from public or private research centers.

L'archive ouverte pluridisciplinaire **HAL**, est destinée au dépôt et à la diffusion de documents scientifiques de niveau recherche, publiés ou non, émanant des établissements d'enseignement et de recherche français ou étrangers, des laboratoires publics ou privés.








Distributed under a Creative Commons Attribution 4.0 International License



## RESEARCH ARTICLE

10.1029/2023JD038712

# Storylines of Sahel Precipitation Change: Roles of the North Atlantic and Euro-Mediterranean Temperature

Paul-Arthur Monerie<sup>1</sup> , Michela Biasutti<sup>2</sup> , Juliette Mignot<sup>3</sup> , Elsa Mohino<sup>4</sup> , Benjamin Pohl<sup>5</sup> , and Giuseppe Zappa<sup>6</sup>

<sup>1</sup>National Centre for Atmospheric Science, Reading, UK, <sup>2</sup>Lamont-Doherty Earth Observatory of Columbia University, Palisades, NY, USA, <sup>3</sup>LOCEAN/IPSL Sorbonne University/IRD/CNRS/MNHN, Paris, France, <sup>4</sup>Dpto. Física de la Tierra y Astrofísica, Facultad Ciencias Físicas, Universidad Complutense de Madrid, Ciudad Universitaria, Madrid, Spain, <sup>5</sup>Centre de Recherches de Climatologie, UMR 6282 Biogéosciences, CNRS/Université de Bourgogne Franche-Comté, Dijon, France, <sup>6</sup>National Research Council of Italy, Institute of Atmospheric Sciences and Climate (CNR-ISAC), Bologna, Italy

### Key Points:

- Future changes in Sahel precipitation are uncertain
- Changes in North Atlantic and Euro-Mediterranean temperatures explain up to 60% of the Sahel precipitation change uncertainty
- Uncertainty in changes in Sahel precipitation is associated with uncertainty in the future northward shift of the Saharan heat low

### Supporting Information:

Supporting Information may be found in the online version of this article.

### Correspondence to:

P.-A. Monerie,  
[p.monerie@reading.ac.uk](mailto:p.monerie@reading.ac.uk)

### Citation:

Monerie, P.-A., Biasutti, M., Mignot, J., Mohino, E., Pohl, B., & Zappa, G. (2023). Storylines of Sahel precipitation change: Roles of the North Atlantic and Euro-Mediterranean temperature. *Journal of Geophysical Research: Atmospheres*, 128, e2023JD038712. <https://doi.org/10.1029/2023JD038712>

Received 15 FEB 2023

Accepted 9 AUG 2023

**Abstract** Future changes in Sahel precipitation are uncertain because of large differences among projections from various models. In order to explore this uncertainty, we use a storyline approach which seeks to identify alternative plausible evolutions of Sahel precipitation and their driving factors. By analyzing projections from the CMIP6 climate models, we show that changes in North Atlantic and in Euro-Mediterranean temperatures explain up to 60% of the central Sahel precipitation change uncertainty. We then construct several storylines of Sahel precipitation change based on future plausible changes in North Atlantic and Euro-Mediterranean temperatures. In one storyline, an amplified warming of both the North Atlantic and the Euro-Mediterranean areas promotes a northward shift of the West African monsoon, increasing precipitation over the central Sahel, while, in the opposite storyline, a moderate warming in both regions is associated with a small change in precipitation over the central Sahel and a decrease in precipitation over the western Sahel, at the end of the 21st century. These results indicate that Sahel precipitation uncertainty will not be substantially reduced unless the uncertainty in the future warming of the North Atlantic and the Euro-Mediterranean areas is constrained.

**Plain Language Summary** Variations in the strength of the West African Monsoon (WAM) circulation have societal impacts on around 80 million people from Senegal to Chad. However, future projections of the WAM precipitation are uncertain for the end of the 21st century because of strong differences from one climate model to another. We show here that sources of uncertainty in Sahel precipitation depend on changes in North Atlantic and Euro-Mediterranean temperature, relative to changes in global mean surface air temperature. We show that differences in how climate models simulate the future warming over the North Atlantic and Euro-Mediterranean area explain a large proportion of the uncertainty in precipitation change over the central Sahel. We provide a method that could be helpful at selecting models for impact studies, based on their sensitivity to climate change over the North Atlantic ocean and Mediterranean Sea.

## 1. Introduction

The West African Monsoon (WAM) brings precipitation in summer to around 80 million people from Senegal to Chad. Variability of the monsoon circulation has large impacts on Sahelian societies: on human health (Cissé, 2019; Jankowska et al., 2012; Ramin and McMichael, 2009), agropastoral activities (Marega et al., 2018), agriculture (Sultan and Gaetani, 2016), and the gross domestic product (Baarsch et al., 2020; Sainte Fare Garnot et al., 2018), among others. Therefore, understanding, predicting, and projecting current and future variations of precipitation across the Sahel is an issue of major importance.

Precipitation has increased over the Sahel since the drought of the 1970s and 1980s (Sanogo et al., 2015). The current understanding attributes the recovery to a combination of factors: a warming of the North Atlantic (Martin & Thorncroft, 2014) and Mediterranean (Park et al., 2016) Sea Surface Temperature (SSTs), an increase in greenhouse gas (GHG) emissions (Dong & Sutton, 2015; Monerie et al., 2022), and a decrease in anthropogenic aerosol emissions from Europe and northern America (Hirasawa et al., 2020; Marvel et al., 2020; Monerie et al., 2022). The future evolution in GHG atmospheric concentration is uncertain (O'Neill et al., 2016). Yet, GHG concentrations are projected to increase until the end of the 21st century in most of the emission scenarios

© 2023. The Authors.

This is an open access article under the terms of the [Creative Commons Attribution License](https://creativecommons.org/licenses/by/4.0/), which permits use, distribution and reproduction in any medium, provided the original work is properly cited.

considered in the IPCC AR6. We thus expect Sahel precipitation to be primarily affected by future changes in GHG concentrations via their effects on surface air temperature and atmospheric circulation.

Multi-model mean projections show an increase in precipitation over the central Sahel and a decrease in precipitation over the Western Sahel (Biasutti, 2013a; Monerie, Wainwright, et al., 2020). This zonal contrast in precipitation change arises from the competitive roles of increases in land surface and SST (Biasutti, 2013b; Gaetani et al., 2017; Monerie, Sanchez-Gomez, et al., 2020; Monerie et al., 2021). Future changes in Sahel precipitation are nevertheless very model dependent in both ensembles of the 5th and 6th phases of the Climate Model Inter-comparison Project (CMIP5 and CMIP6; Taylor et al., 2012; Eyring et al., 2016). The inter-model spread in precipitation change is higher than the multi model mean change itself over a large part of West Africa (Monerie, Wainwright, et al., 2020) implying that even the direction of change is uncertain. Uncertainty in Sahel precipitation change primarily comes from differences among climate models in their projected atmospheric circulation patterns (Monerie, Wainwright, et al., 2020), and from uncertainty in future changes of the WAM circulation tied to uncertainty in the simulation of temperature changes over the Northern Hemisphere (Monerie et al., 2021; Park et al., 2015). The uncertainty in Sahel precipitation was especially tied to that over the Mediterranean SSTs in the sensitivity experiments by Park et al. (2016), when they imposed temperature increases of different magnitudes over the Northern Hemisphere and over separate oceanic basins, in the same climate model. They showed that the warming of the North Atlantic Ocean also contributes to the increase in Sahel precipitation.

In addition to simulating different patterns in SST, CMIP6 climate models simulate a large range of changes in global mean surface air temperature (O'Neill et al., 2016). Yet, Monerie, Wainwright, et al. (2020) showed that the inter-model spread in global mean surface temperature only explains a small proportion of the inter-model spread in Sahel precipitation change.

Because of strong uncertainty, projections of future changes in Sahel precipitation do not provide useful and reliable information to the decision makers developing adaptation strategies in the region. Within the ultimate goal of reducing uncertainty, we aim at improving our understanding of drivers of Sahel precipitation, focusing on mechanisms that explain differences among models' projections. Previous works suggested that uncertainty in Sahel precipitation is primarily due to how models simulate future changes of the atmospheric circulation (Monerie, Wainwright, et al., 2020). We hence hypothesize that we can document sources of Sahel precipitation uncertainty focusing on drivers of the WAM circulation.

We use a storyline approach (Zappa and Shepherd, 2017) to document and represent uncertainty in future changes in Sahel precipitation. This is done by developing storylines, akin to response scenarios for a given forcing, that span the projections from an ensemble of climate models and that provide physically self-consistent future evolutions of global and regional climate. The basis for the construction of these storylines is the remote drivers of the circulation response. The storyline approach has been applied to Europe (Zappa and Shepherd, 2017) and several regions of the Southern Hemisphere (Mindlin et al., 2020). Here, we apply it to future changes in precipitation over the Sahel, targeting the projections by a large number of CMIP6 models under one emission scenario.

In Section 2, we introduce the data set used in this paper, detail the indices used to represent the Sahel changes and its possible drivers, and provide a succinct introduction to the implementation of the storyline approach and to the decomposition of precipitation into thermodynamically and dynamically forced components. In Section 3, we motivate the selection of the Euro-Mediterranean and North Atlantic surface temperature regional means as the remote drivers of the WAM on which the storylines are constructed. In Section 4 we construct the storylines and show the range of projections that can be encompassed by chosen warming levels for each driver. Section 5 introduces the alternative approach of spanning the uncertainty by choosing subsets of the CMIP6 ensemble based on where they lay in the phase space of drivers' warming and we confirm that the range of Sahel precipitation response is explained by a range of circulation responses. We conclude the paper with a short summary and discussion.

## 2. Data and Methods

### 2.1. Simulations

We use historical and scenario simulations from 43 ocean-atmosphere coupled general circulation models (AOGCMs) that participated to CMIP6 (Table S1 in Supporting Information S1). The historical simulations

cover the 1850–2014 period and are forced by reconstructions of external forcings, for example, greenhouse gases, anthropogenic aerosols, solar cycle, volcanic activity over the historical period (Eyring et al., 2016). For the 2015–2100 period, we use the SSP5-8.5 high-emissions scenario (O'Neill et al., 2016), in which GHG emissions lead to a radiative imbalance at the top of the atmosphere of approximately  $8.5 \text{ W m}^{-2}$  at the end of the 21st century. We have used one ensemble member for each model, relying on the fact that uncertainty in the Sahel response by 2100 is massively explained by differences between climate models, rather than internal variability (Monerie, Wainwright, et al., 2020).

The effect of climate change is assessed by comparing precipitation and temperature of the late 21st century (period 2060–2099) to the late 20th century (1960–1999). The 1960–1999 historical period is chosen to sample both the drought of the 1970s–1980s and the wetter 1960s. We use summer-mean (from July to September, JAS) anomalies.

## 2.2. Indices

Because we focus on the uncertainty created by the pattern of warming, all indices are scaled by global warming level, defined as the change in global mean surface air temperature ( $\Delta T$ ) over the same periods and as simulated by each model. Below we detail the regional means defining individual indices.

### 2.2.1. Sahel Precipitation

As explained above, multi-model mean estimates of future changes in Sahel precipitation project onto a zonal contrast in precipitation change (Monerie, Sanchez-Gomez, et al., 2020), with a decrease in precipitation over the western Sahel and an increase in precipitation over the central Sahel. We define two precipitation indices to account for this regional heterogeneity in precipitation change. The western Sahel precipitation index is obtained by averaging precipitation between  $20^\circ\text{W}$  and  $5^\circ\text{W}$ , and from  $10^\circ\text{N}$  to  $20^\circ\text{N}$ . The central Sahel precipitation index is defined as the average of precipitation between  $5^\circ\text{W}$  and  $20^\circ\text{E}$  and between  $10^\circ\text{N}$  and  $20^\circ\text{N}$ , as in Monerie, Sanchez-Gomez, et al. (2020).

### 2.2.2. Temperature Indices

The choice of the potential remote drivers of uncertainty in Sahel precipitation change analyzed here is motivated by the analysis presented in Figure 1, and discussed in Section 3. Unless specified differently, averages are computed over both oceanic and land areas. These potential drivers are:

- The North Atlantic Ocean (NATL), defined as the regional mean of surface air temperature, from  $60^\circ\text{W}$  to  $0^\circ\text{E}$  and from  $20^\circ\text{N}$  to  $60^\circ\text{N}$ , considering ocean grid points only. The change in this index from the late 20th Century to the late 21st Century is denoted as  $\Delta T_{\text{NATL}}$ .
- The Euro-Mediterranean region (MED), defined as the average of the surface air temperature from  $0^\circ\text{E}$  to  $40^\circ\text{E}$  and from  $30^\circ\text{N}$  to  $50^\circ\text{N}$ . Its change is denoted as  $\Delta T_{\text{MED}}$ .
- The inter-hemispheric temperature gradient, defined as the difference between the area-averaged temperature between the Northern Hemisphere ( $0^\circ\text{N}$ – $87.5^\circ\text{N}$ ) and the Southern Hemisphere ( $87.5^\circ\text{S}$ – $0^\circ\text{N}$ ).
- The Northern Hemisphere temperature relative to the tropics, defined as the difference between the mean surface air temperature in  $20^\circ\text{N}$ – $75^\circ\text{N}$  relative to the mean in  $20^\circ\text{S}$ – $20^\circ\text{N}$  (Park et al., 2015).
- The northern Pacific surface air temperature, defined as the area average from  $30^\circ\text{N}$  to  $60^\circ\text{N}$  and from  $150^\circ\text{E}$  to  $240^\circ\text{E}$ , considering ocean grid points only.
- The polar amplification, defined as the polar cap mean surface air temperature change in  $60^\circ\text{N}$ – $90^\circ\text{N}$ , following Manzini et al. (2014).
- The temperature of the Saharan desert, defined as the region between  $20^\circ\text{N}$  and  $30^\circ\text{N}$  and between  $30^\circ\text{W}$  and  $30^\circ\text{E}$ , over land only.

### 2.2.3. Location of the Saharan Heat Low

Meridional shifts of the Saharan Heat Low (SHL) have strong effects on Sahel precipitation, with a northward shift of the SHL typically associated with an increase in Sahel precipitation (Dixon et al., 2017, 2018; Lavaysse et al., 2009; Shekhar and Boos, 2017).

We define an index that documents the meridional location of the SHL. The index is based on the low-level atmospheric thickness (LLAT; Lavaysse et al., 2009), that is the difference between geopotential height ( $Z$ ) at

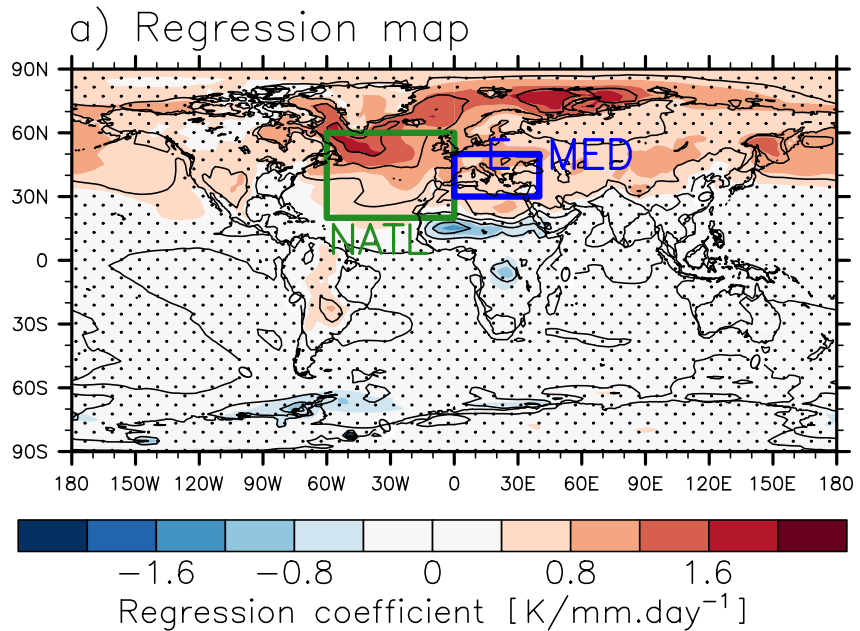


**Figure 1.** Regression coefficients [ $\text{K}/\text{mm d}^{-1}$ ], between changes in surface air temperature and in Sahel precipitation (central Sahel precipitation in color and western Sahel precipitation with contours), across the CMIP6 ensemble (See Table S1 in Supporting Information S1). Changes in Sahel precipitation and temperature are defined as the difference between the period 2060–2099 under the SSP5-8.5 emission scenario and the period 1960–1999 under the historical scenario, in July–September. Contours range from  $-2$  to  $+2$ , every  $0.5 \text{ K}/\text{mm d}^{-1}$ . Stippling indicates that the regression coefficient is not significant at the 5% level according to a Student's  $t$  test, for the central Sahel. The green box indicates the area that is used to compute the NATL index and the blue box indicates the area that is used to compute the Euro-Mediterranean index.

700 hPa and 925 hPa (i.e.,  $\text{LLAT} = \text{Z}700\text{--Z}925$ ). The latitudinal location of the SHL is then defined as the latitude of the maximum of the LLAT sector zonal mean. We only consider LLAT values that lie between  $15^\circ\text{W}$  and  $30^\circ\text{E}$  and from  $0^\circ\text{N}$  to  $40^\circ\text{N}$ . We smooth the LLAT values performing a cubic splines interpolation before defining the latitudinal location of the SHL (Shekhar and Boos, 2017).

### 2.3. Storyline Approach

We estimate the epochal change between the recent (1960–1999) and future (2060–2099) climate, for a given field  $V$ , with a pattern scaling approach following Tebaldi and Arblaster (2014). For a location  $x$  and a model  $m$ :

$$\Delta V_{xm} = \Delta T_m R_{xm}, \quad (1)$$

where  $\Delta T$  is the change in global mean surface air temperature and  $R$  the climate response pattern.

The pattern  $R_{xm}$  is then modeled as a linear combination of the response to a number of remote drivers, scaled by  $\Delta T$  and standardized (Zappa and Shepherd, 2017). Given a pair of remote drivers, as in this study, we estimate  $R_{xm}$  as follows:

$$R_{xm} = a_x + b_x \left( \frac{\Delta T_{\text{Driver1}}}{\Delta T} \right)'_m + c_x \left( \frac{\Delta T_{\text{Driver2}}}{\Delta T} \right)'_m + e_{xm}, \quad (2)$$

where primes ( $'$ ) indicate that the changes of the remote drivers are standardized using the CMIP6 ensemble mean and standard deviation. The coefficients  $a_x$ ,  $b_x$ , and  $c_x$  are obtained using a multiple linear regression across the model ensemble. With this fit,  $a_x$  is the response that is expected with no change of the drivers with respect to the multi model mean.  $b_x$  and  $c_x$  are the sensitivity of  $R_{xm}$  to the anomalies (with respect to the multi-model mean) of the two remote drivers, scaled by  $\Delta T$ .  $e_{xm}$  is the residual that is not captured by the linear expansion and is associated with changes that are due to external forcing and effect of internal climate variability, but that are not associated with the response of the two remote drivers. We show that  $e_{xm}$  can be large but that the regression framework is still a useful methodology for estimating changes in precipitation (Figure S1 in Supporting Information S1).

From Equations 1 and 2, the change of a given field, per unit of  $\Delta T$ , is finally obtained as:

$$\frac{\Delta V_{xm}}{\Delta T_m} = a_x + b_x \left( \frac{\Delta T_{Driver1}}{\Delta T} \right)'_m + c_x \left( \frac{\Delta T_{Driver2}}{\Delta T} \right)'_m + e_{xm}. \quad (3)$$

#### 2.4. Decomposing Precipitation Anomalies

We estimate the thermodynamic and dynamic components of precipitation change following Chadwick et al. (2013). The decomposition method assumes that precipitation is primarily convective in the tropics and that precipitation can be approximated by,

$$P = M^* q \text{ and thus } \Delta P = \Delta(M^* q) \quad (4)$$

Where  $P$  is precipitation,  $M^*$  is a proxy for convective mass flux, from the boundary layer to the free troposphere, and  $q$  is near-surface specific humidity.  $P$ ,  $M^*$ , and  $q$  are computed for each grid point, with  $M^*$  obtained from model data as  $P/q$ .  $\Delta$  indicates the epochal change in precipitation, as defined in Section 2.2. An increase in precipitation is associated with either an increase in near-surface specific humidity, a strengthening of the convective mass flux, or both. We can then reformulate precipitation changes in terms of thermodynamic ( $\Delta P_{therm}$ ), dynamic ( $\Delta P_{dyn}$ ) and cross nonlinear ( $\Delta P_{cross}$ ) components.

$$\Delta P = M^* \Delta q + q \Delta M^* + \Delta q \Delta M^*. \quad (5)$$

In other words,

$$\Delta P = \Delta P_{therm} + \Delta P_{dyn} + \Delta P_{cross}. \quad (6)$$

Sahel precipitation change uncertainty is primarily due to  $\Delta P_{dyn}$  (Monerie, Wainwright, et al., 2020), which we can decompose into an anomaly associated with the effect of climate change on a future weakening of the large-scale tropical circulation  $\Delta P_{weak}$ , and with a change in the pattern of the circulation  $\Delta P_{shift}$ , following Chadwick et al. (2016) as,

$$\Delta P_{dyn} = \Delta P_{weak} + \Delta P_{shift}, \quad (7)$$

where

$$\Delta P_{weak} = q \Delta M^*_{weak}, \quad (8)$$

and

$$\Delta P_{shift} = q \Delta M^*_{shift}. \quad (9)$$

$\Delta M^*_{weak}$  is the change in mass flux that is associated with a change of the strength of the mean tropical circulation. Chadwick et al. (2013) and (Held & Soden, 2006) show that this change is proportional to the climatological mass-flux field, and thus,

$$\Delta M^*_{weak} = -\alpha M^*, \quad (10)$$

with

$$\alpha = - \left( \frac{\text{tropical mean } \Delta M^*}{\text{tropical mean } M^*} \right). \quad (11)$$

The tropical mean is here the average between 30°S and 30°N.

Finally,  $\Delta M^*_{shift}$  is computed as the residual between  $\Delta M^*$  and  $\Delta M^*_{weak}$ :

$$\Delta M^*_{shift} = \Delta M^* - \Delta M^*_{weak}. \quad (12)$$

The decomposition is performed using monthly means prior to computing the seasonal means and before averaging over the 40 years period.

### 3. Drivers of Uncertainty in Sahel Precipitation Change

Figure 1 shows the regression coefficient of the changes in surface air temperature against the changes in summer Sahel precipitation for the end of the 21st century, across CMIP6 models. Simulated uncertainty in changes in western and central Sahel precipitation is associated with uncertainty in future changes in temperature over the Northern Hemisphere, as shown in Park et al. (2015) for CMIP5. This pattern of SST is different from the one typically associated with the observed variations of Sahel precipitation at seasonal to multi-decadal scales. The latter shows larger anomalies in the tropical oceans and subsumes the influence of ENSO in the East Pacific, the dipole mode in the Atlantic, and the interhemispheric gradient. In contrast, Figure 1 shows that larger projected warming over the North Pacific, North Atlantic, Mediterranean, Arctic temperature, and over northern Africa and Europe is associated with a greater degree of Sahel wetting in simulations of the 21st century.

Within the large region identified by the regression analysis as associated with disagreement across the CMIP6 models, we select two sub-regions to function as Sahel drivers in the storyline approach based on the following criteria. First, they have a strong effect on Sahel precipitation, as identified in the literature from observed statistics and from modeling studies that provide a mechanistic explanation. Second, their variations across models are, as much as possible, independent; this is necessary in order to span as much inter-model variations as possible with the least number of drivers.

The first criterion leaves as possible choices the North Atlantic and the Euro-Mediterranean area— which are correlated to the Sahel in observations (Giannini et al., 2013; Rowell, 2003) and have been shown to affect the temperature and humidity advected into the monsoon region (Liu et al., 2014)— and the extra-tropical zonal mean, which has been linked to the energetic imbalance that shifts the ITCZ (e.g., Schneider et al., 2014). The same criterion leads us to exclude the North Pacific and the Arctic, which have not been linked to Sahel precipitation variability other than by their contribution to the interhemispheric gradient. The surface temperature over North Africa has been invoked as a possible driver of Sahel precipitation through its effect on the Sahara Heat Low (Lavaysse et al., 2009; Mutton et al., 2022), but the correspondence between the Saharan temperature and the Sahel precipitation is weak (Biasutti et al., 2008, Figure 2), leading us to exclude it from the candidate list.

Among the candidates that passed the first criterion, the two drivers that exhibit the weakest correlation coefficient with each other are the north Atlantic and the Euro-Mediterranean warming. The inter-model correlation between  $\frac{\Delta T_{\text{NATL}}}{\Delta T}$  and  $\frac{\Delta T_{\text{MED}}}{\Delta T}$  is 0.35 (Figure 2) indicating that only ~12% of the temperature variance across models is not independent in the two regions. The inter-hemispheric temperature gradient is instead highly correlated with both the North Atlantic and Mediterranean warming, implying that it cannot be used to create storylines in conjunction with these regional drivers, but it could be used a simple single driver. An application of this simpler approach is discussed in Supporting Information S1.

Drivers other than surface temperature could be selected, such as the Sahara Heat Low. Climate change leads to a northward shift of the SHL (e.g., Monerie, Sanchez-Gomez, et al., 2020; Monerie, Wainwright, et al., 2020, among others), favoring an increase in precipitation over the Sahel (Biasutti et al., 2009; Dixon et al., 2017; Lavaysse et al., 2016; Roehrig et al., 2011; Shekhar and Boos, 2017) (Figure 2). Indeed, the uncertainty in the simulated change in the latitude of the SHL is highly correlated with the uncertainty in Sahel precipitation both in the West and the Central Sahel (Figure 2). Yet, this quantity is well correlated with both the Euro-Mediterranean ( $r = 0.72$ ) and the North Atlantic ( $r = 0.57$ ) temperature, with both correlations significant at the 1% level. Moreover, it is still unclear if the location of the SHL ought to be considered an external driver to Sahel precipitation, or if it is part of a tightly coupled system. For these reasons, we do not select the uncertainty in the location of the SHL for the storyline approach. Instead, we select the North Atlantic and Euro-Mediterranean temperature indices as drivers and assume that the effect of uncertainty in future changes in the location of the SHL is already included in the ensuing storylines, given that these drivers affect the Sahel by shifting the SHL northwards (Martin & Thorncroft, 2014; Rowell, 2003).

The inter-model spread in temperature change is high over the North Atlantic Ocean with projections ranging from a decrease to an increase in temperature over the Atlantic subpolar gyre (Swingedouw et al., 2021). The positive regression coefficients over this region in Figure 1 are consistent with previous results highlighting the significant influence of North Atlantic SSTs anomalies, as the ones related to the Atlantic Multidecadal Variability (AMV), on Sahel precipitation (e.g., Mohino et al., 2011). A positive phase of the AMV, that is, a warmer than usual North Atlantic ocean, is indeed associated with anomalously high precipitation over the Sahel (and

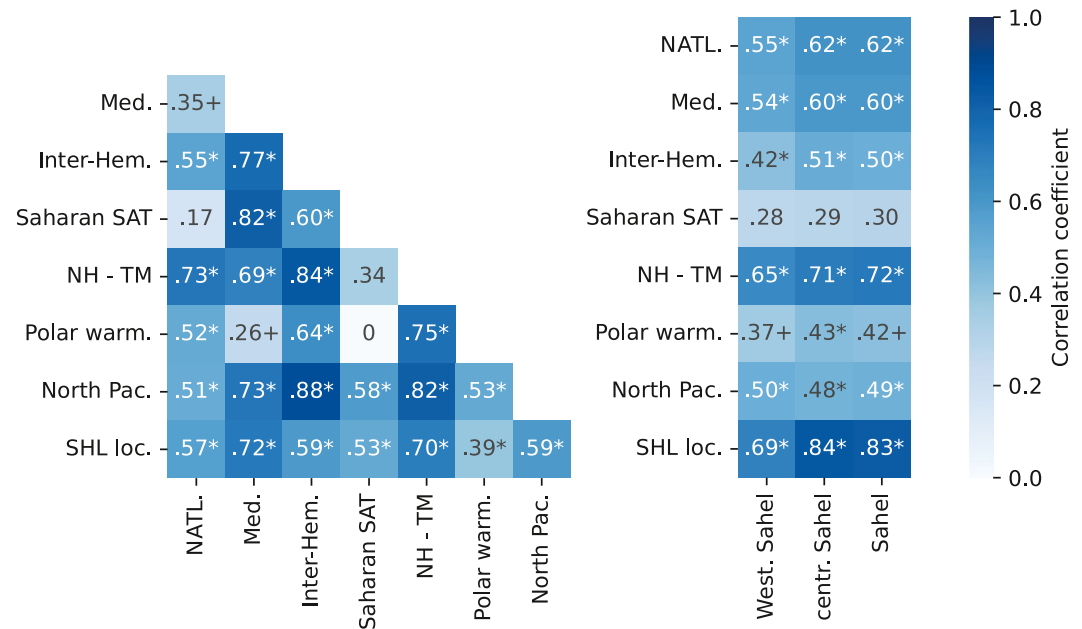


**Figure 2.** (left) Correlation coefficient between the projected changes in eight climate indices, here selected as possible drivers of Sahel precipitation, scaled by  $\Delta T$  across CMIP6 models. (right) Correlation coefficient between the projected changes in the climate indices and the change in the western, central and entire Sahel ( $10^{\circ}\text{W}$ – $10^{\circ}\text{E}$ ) precipitation, across CMIP6 models. A star (plus) indicates that the correlation coefficient is significant at the 1% (5%) level. NATL stands for North Atlantic Ocean temperature, Med is the temperature averaged over the Euro-Mediterranean area, Inter-Hem is the inter-hemispheric temperature gradient, Saharan SAT is for the temperature averaged over the Sahara desert, NH-TM is the Northern Hemisphere temperature relative to the tropics, Polar warm stands for the polar amplification, North Pac is the temperature averaged over the northern Pacific Ocean. Saharan Heat Low (SHL) loc stands for the location ( $^{\circ}\text{North}$ ) of the SHL. See Section 2.2.2 for the definition of the indices.

vice-versa) in both observations and simulations (Mohino et al., 2011; Monerie et al., 2019). A possible role of the North Atlantic SSTs in future changes in Sahel precipitation was established in previous work (Bellomo et al., 2021; Monerie, Wainwright, et al., 2020; Park et al., 2016; Swingedouw et al., 2021). We confirm here, using a multiple linear regression framework, that models that simulate the strongest warming of the North Atlantic Ocean, relative to the global mean surface temperature change, also simulate stronger increases in Sahel precipitation (Figure 3a).

Anomalously high temperature of the Mediterranean Sea is also associated with an increase in Sahel precipitation, in both observations and simulations (Fontaine et al., 2010; Rowell, 2003). The warming of the Mediterranean Sea is associated with a warming of the Sahara desert (Figure S2 in Supporting Information S1) and a strengthening of the northerly moisture flux (Rowell, 2003) that allow Sahel precipitation to increase. Warming of the Mediterranean Sea, due to climate change, was also found to be associated with an increase in precipitation over the Sahel (Park et al., 2016). Figure 3b confirms that changes in Sahel precipitation are sensitive to the increase in temperature over the Euro-Mediterranean region.

We note that Figure 1 shows negative regression coefficient over the Sahel, which is consistent with precipitation affecting local surface temperature: enhanced Sahel precipitation cools the surface through increased moisture availability and enhanced latent heat flux and through an enhanced cloud cover that reduces net surface shortwave radiation.

## 4. Uncertainty Due To the Remote Drivers

### 4.1. Constructing the Storylines

We express uncertainty in changes in precipitation as a function of uncertainty in changes in North Atlantic and Euro-Mediterranean surface air temperature (Equation 3). We show that this framework allows explaining up to 60% of the uncertainty in precipitation change of the CMIP6 ensemble (Figure 4). We then explore the



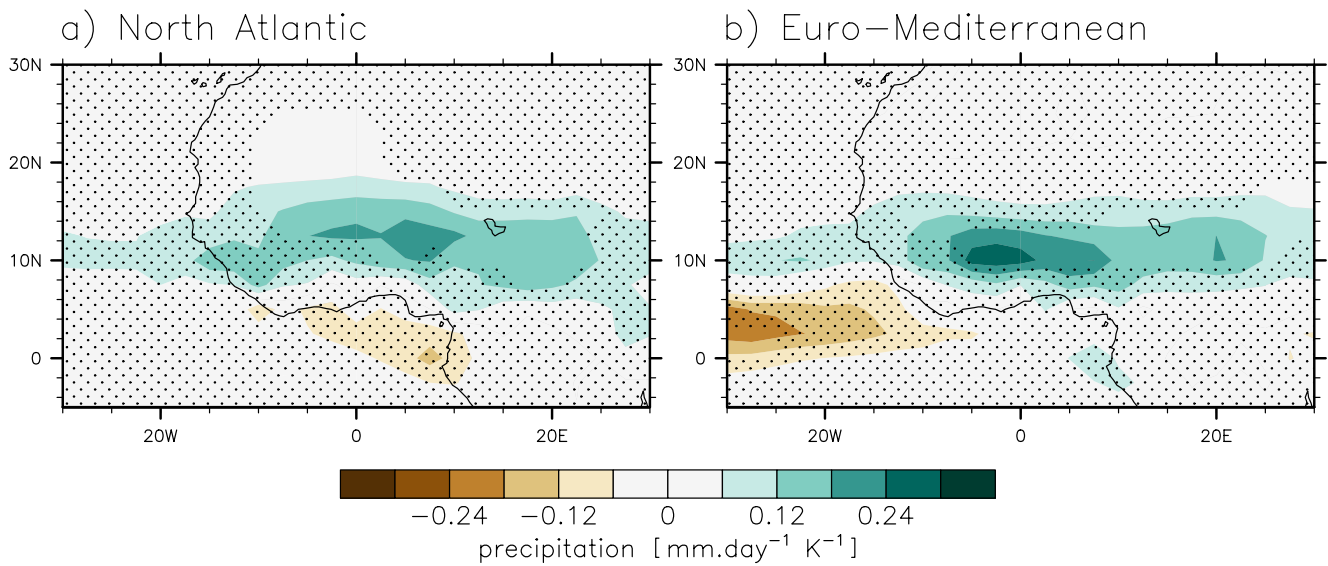


**Figure 3.** Sensitivity of the projected changes in precipitation [ $\text{mm day}^{-1} \text{K}^{-1}$ ] to the uncertainty in the magnitude of the (a) North Atlantic warming ( $b_x$ ) and of (b) the Euro-Mediterranean warming ( $c_x$ ).  $b_x$  and  $c_x$  are estimated with a multiple linear regression, following Equation 3. Stippling indicates that regression values are not significant at the 5% level according to a Student's  $t$  test.

uncertainty associated with the drivers, by constructing different storylines of Sahel precipitation change depending on the changes in North Atlantic and Euro-Mediterranean temperature.

The effects of anomalously high and low warming of the North Atlantic and Euro-Mediterranean regions on a variable  $V$  are defined using the regression coefficients from Equation 2 and displayed in Figure 3,  $b_x$  for the North Atlantic and  $c_x$  for the Euro-Mediterranean area.

The storylines are then constructed using a scenario index  $i$ , following Zappa and Shepherd (2017), as:

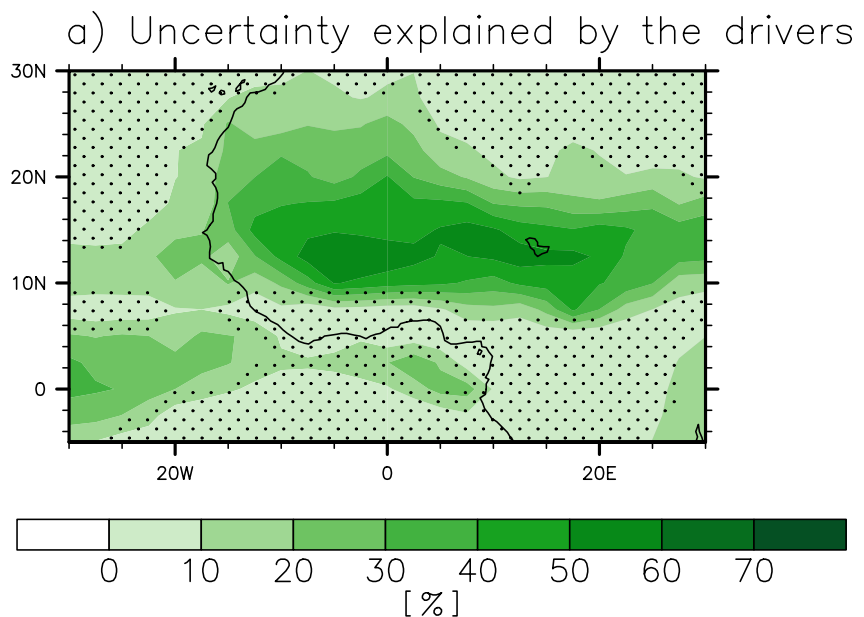


**Figure 4.** Fraction of the uncertainty, that is, variance, in the precipitation response to climate change that is explained by the uncertainty in the response of the remote drivers and by global warming ( $r^2$  defined from the CMIP6 inter-model spread and  $\Delta T_m \left[ a_x + b_x \left( \frac{\Delta T_{\text{NATL}}}{\Delta T} \right)'_m + c_x \left( \frac{\Delta T_{\text{MED}}}{\Delta T} \right)'_m \right]$ ) (from Equation 3) at the end of the 21st century. Stippling indicates where the correlation coefficient is not significant at the 5% level.

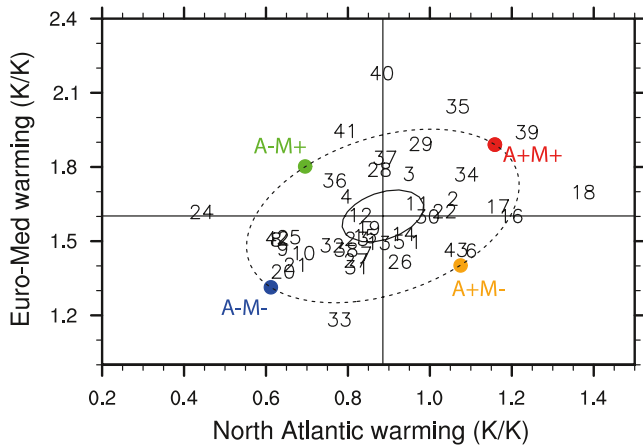


**Figure 5.** Changes in Euro-Mediterranean temperature ( $\frac{\Delta T_{MED}}{\Delta T}$ ) and North Atlantic temperature ( $\frac{\Delta T_{NATL}}{\Delta T}$ ), scaled by global-mean warming ( $K K^{-1}$ ). Each CMIP6 model is shown by its number (See Table S1 in Supporting Information S1). The outer ellipse marks the 80% confidence region of the CMIP6 model distributions, assuming the responses in the two drivers follow a bivariate normal distribution with an across-model correlation coefficient ( $r$ ) between  $\frac{\Delta T_{NATL}}{\Delta T}$  and  $\frac{\Delta T_{MED}}{\Delta T}$  equal to 0.35. The inner ellipse delimitates models that have low anomalies relative to the multi-model mean, that is, when the combined standardized anomaly in the driver response is smaller than 0.5. for example,  $\sqrt{\left[\left(\frac{\Delta T_{NATL}}{\Delta T}\right)'_m\right]^2 - 2r\left(\frac{\Delta T_{NATL}}{\Delta T}\right)'_m\left(\frac{\Delta T_{MED}}{\Delta T}\right)'_m + \left[\left(\frac{\Delta T_{MED}}{\Delta T}\right)'_m\right]^2} < 0.5$ , following (Mindlin et al., 2020). Vertical and horizontal lines denote the multi-model mean changes in Euro-Mediterranean and North Atlantic temperature. The four storylines (A+M+, A-M-, A+M-, A-M+) are selected on the confidence ellipse so that they reflect equal standardized anomalies in each driver (see Supporting Information S1 for details).

$$\frac{\Delta V_x}{\Delta T} = a_x \pm ib_x \pm ic_x. \quad (13)$$

Figure 5 shows the change in North Atlantic ( $\frac{\Delta T_{NATL}}{\Delta T}$ ) and Euro-Mediterranean ( $\frac{\Delta T_{MED}}{\Delta T}$ ) surface air temperature, scaled by changes in global mean surface air temperature, for each CMIP6 climate model. There is a large inter-model spread in both drivers (Figure 5). We show that the North Atlantic warming can be faster or slower than global mean warming, while the Euro-Mediterranean area can warm up to twice as fast as the global mean warming. We then construct four extreme, but plausible, storylines of Sahel precipitation change, with each reflecting different combinations of future warming of the North Atlantic and Euro-Mediterranean areas.

To account for the weak correlation between the two indices ( $r = 0.35$ ), we define the scenario index following Mindlin et al. (2020) (See the Supporting Information S1). This approach implies using a different scenario index for the storylines with same-signed changes in the drivers (A+M+ and A-M-) and the storylines with opposite changes in drivers (A+M- and A-M+), with,

$$i = i_1, \text{ and}$$

$$i_1 = \sqrt{\frac{(1-r^2)}{2(1-r)}} \chi^2(0.8; 2) \sim 1.46, \quad (14)$$

for A+M+ and A-M-, and,

$$i = i_2, \text{ and}$$

$$i_2 = \sqrt{\frac{(1-r^2)}{2(1+r)}} \chi^2(0.8; 2) \sim 1.01, \quad (15)$$

for A+M- and A-M+.

$\chi^2(k, p)$  is the quantile function of the chi-squared distribution with  $k$  degrees of freedom evaluated at probability  $p$ . The values are chosen so that the anomalies in the two driver responses are selected to lie on the 80% confidence region of the joint CMIP6 distribution (see for instance Figure 5 for the temperature indices).

A+M+ is the storyline for which North Atlantic and Euro-Mediterranean temperatures increase more strongly than the global mean surface air temperature, and relative to the CMIP6 ensemble mean (Table S2 in Supporting Information S1). A-M- is the opposite storyline, for which North Atlantic and Euro-Mediterranean temperatures increase more weakly than the ensemble-mean. A+M- and A-M+ are the storylines where North Atlantic temperature increases strongly and Euro-Mediterranean temperature increases weakly, and vice versa, all relative to the increase in global mean surface air temperature and to the CMIP6 ensemble. Figure 5 shows that all four storylines lie within the CMIP6 ensemble spread and are thus associated with plausible changes in North Atlantic and Euro-Mediterranean temperature.

#### 4.2. Effects of the Storylines on Changes in Precipitation

Figure 6a shows the effect of climate change, scaled by  $\Delta T$ , on precipitation. The multi-model mean forced response is associated with an increase in precipitation over the central Sahel and a small decrease in precipitation over the western Sahel (Figure 6a), as shown in Monerie, Wainwright, et al. (2020), among others. The pattern of precipitation change indicates that the monsoon is projected to strengthen and shift northward toward the end of the 21st century over the central Sahel and to weaken and to shift southward over the western Sahel and the tropical Atlantic Ocean (Figure 6a).

The A+M+ storyline shows a stronger increase in precipitation over land than the multi-model mean. The decrease in western Sahel precipitation is considerably reduced and it largely turns into a wetting of the region

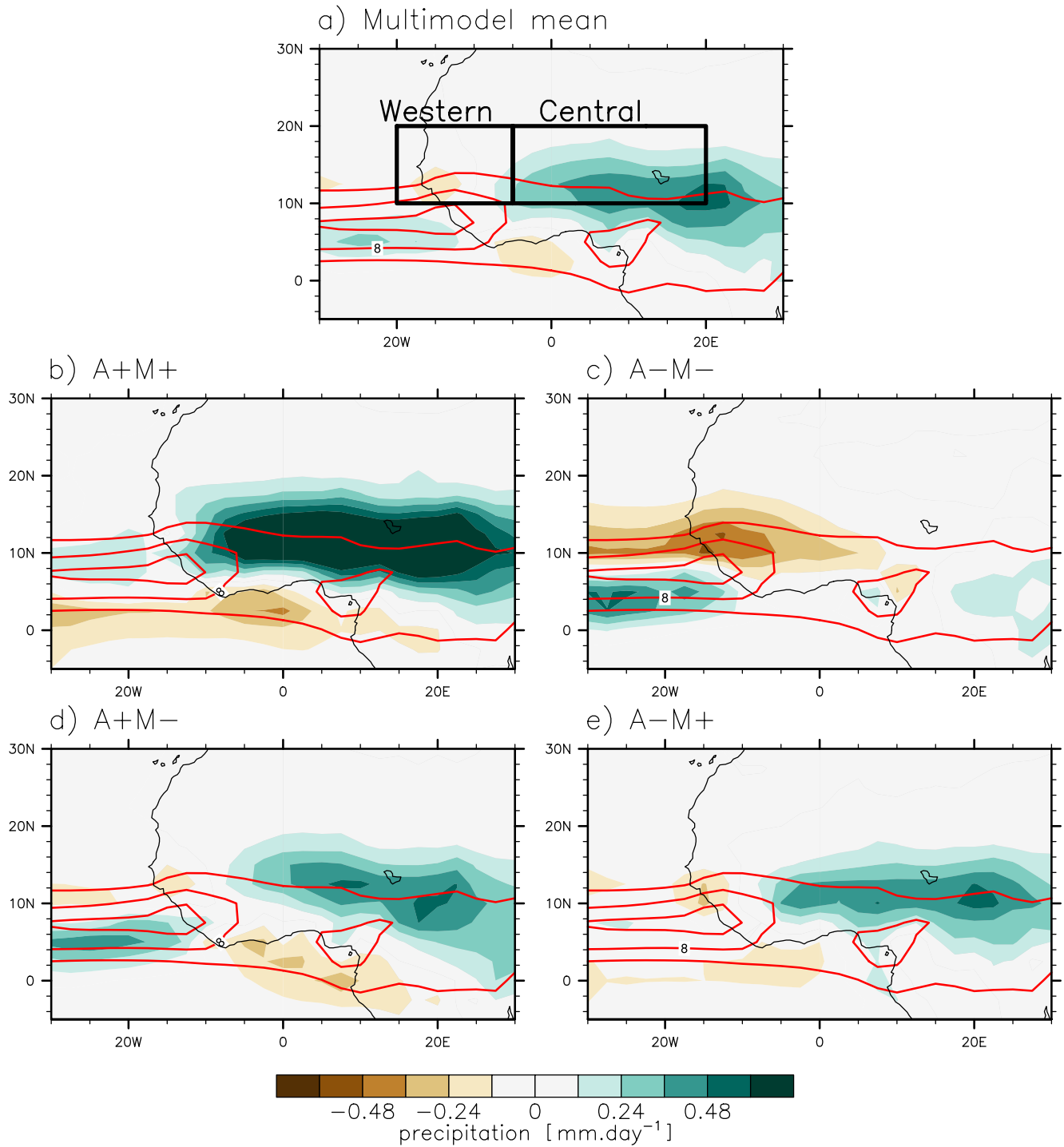


**Figure 6.** Changes in precipitation scaled by  $\Delta T$  [ $\text{mm day}^{-1} \text{K}^{-1}$ ] for the end of the 21st century and for the (a) multi model mean (SSP5.8-5 minus historical simulations) and the four scenarios (b) A+M+, (c) A-M-, (d) A+M- and (e) A-M+. The black boxes in Figure 5a show the areas that were used to define the western and central Sahel precipitation indices. Red contours indicate the climatological precipitation in JAS over 1960–1999 for the CMIP6 ensemble mean (historical simulations).

(Figure 6b). In contrast to the multi-model mean, the South-North dipole in precipitation indicates that the WAM strengthens and shifts northward, over land and over the tropical Atlantic Ocean (Figure 6b). In A-M-, no change in precipitation is found over the central Sahel, while precipitation decreases strongly over the western Sahel. The two opposite storylines thus have strong impacts on Sahel precipitation change, with A+M+ and

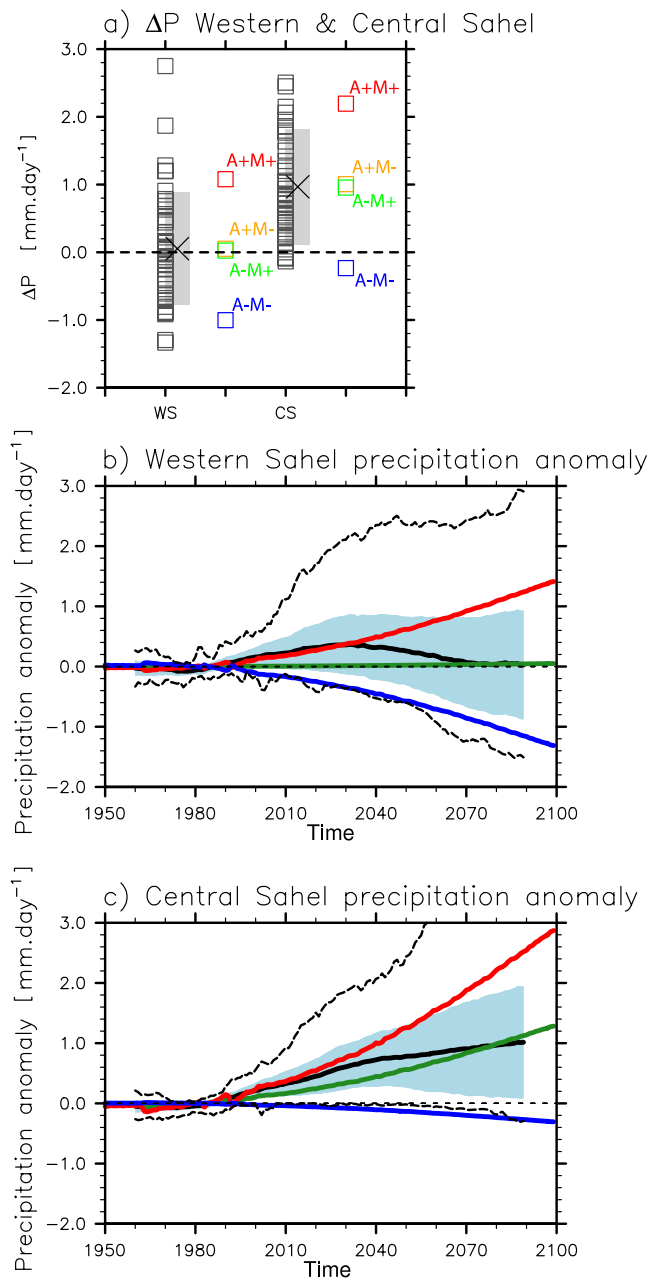


**Figure 7.** (a) Changes in central and western Sahel precipitation for each CMIP6 model (black) and the four scenarios (colors) at the end of the 21st century in SSP5-8.5. The CMIP6 ensemble mean is shown with a black cross and the multi model mean plus and minus one standard deviation by the gray shading. Changes in (b) western and (c) central Sahel precipitation for the CMIP6 ensemble mean (black), the pattern scaling method applied to the multi-model mean precipitation change (green), and the A+M+ (red) and A-M- (blue) scenarios. The CMIP6 spread (multi model mean plus and minus one standard deviation) is shown by the blue shading. Dashed lines show the maximum and minimum values in precipitation anomaly across the CMIP6 ensemble. A 21-year running mean was applied to filter out the high frequency variability for the CMIP6 models. Anomalies are relative to the 1960–1999 period.

A-M- portraying different futures: a substantial increase in precipitation in the former and an increase in the likelihood of drought conditions in the latter.

Uncertainties in changes in North Atlantic and Euro-Mediterranean temperature are associated with similar uncertainty (both in intensity and sign) in Sahel precipitation (Figures 3a and 3b). As a result, a storyline with a high increase in Atlantic temperature and a low increase in Euro-Mediterranean temperature (A+M-) shows changes in precipitation that are similar to both the ensemble mean (Figures 6a and 6d) and to the A-M+ storyline (Figures 6d and 6e).

We show that the four storylines as defined above allow sampling uncertainty in Sahel precipitation change at the end of the 21st century (Figure 7a). A+M- and A-M+ show results that are close to the CMIP6 multi-model mean, and A+M+ and A-M- are extreme storylines but are not outliers, since these storylines lie within the CMIP6 distribution (Figure 7a). A+M+ and A-M- are plausible storylines in precipitation change for the end of the 21st century and provide the strongest difference to the multi model mean. In the remainder of the study we then mostly focus on A+M+ and A-M- storylines.

### 4.3. Time Evolution of the Changes in Sahel Precipitation

We now assess the effects of the two selected storylines on the time-evolving changes in Sahel precipitation, across both the 20th and the 21st centuries. This is done by using Equation 13 but as a function of  $\Delta T$ :

$$\Delta V_x = \Delta T[a_x \pm i(b_x \pm c_x)]. \quad (16)$$

The storyline index  $i$ , and the regression coefficients  $a_x$ ,  $b_x$ , and  $c_x$  are kept constant. We obtain a time evolution of  $\Delta V_x$ , using Equation 16 and with  $\Delta T$ —here given by the multi-model mean global mean warming—that varies from 1 year to another. We computed changes in precipitation for each grid point before deriving the western and central precipitation indexes. We show that the CMIP6 western and central Sahel precipitation change distribution (ensemble-mean and ensemble spread) does not fall well between the A+M+ and A-M- storylines before the mid-21st century (Figures 7b and 7c), showing limitations in this reconstruction of the time-evolution of Sahel precipitation change.

We assume the inability of the storylines to capture the early 21st century CMIP6 Sahel precipitation change uncertainty to be an inherent issue of the pattern scaling method we use. We test this hypothesis by trying to reconstruct the time evolution of the multi-model mean precipitation response (black line) by scaling the end-of century multi-model mean precipitation change based on the time-evolution of the mean  $\Delta T$  (green line) (more details in the Supporting Information S1). The pattern scaling (Figures 7b and 7c) does not allow reproducing the multi-model mean change in Sahel precipitation from the 2000s to the 2030s, and particularly over the western Sahel (Figures 7b and 7c). We suggest this to be due to the fact that the method does not account for the effects of global emissions in anthropogenic aerosols, which were shown to modulate Sahel precipitation over the historical period (e.g., Herman et al., 2020; Monerie et al., 2022; Ndiaye et al., 2022). In addition, the difference between the simulated change in Sahel precipitation

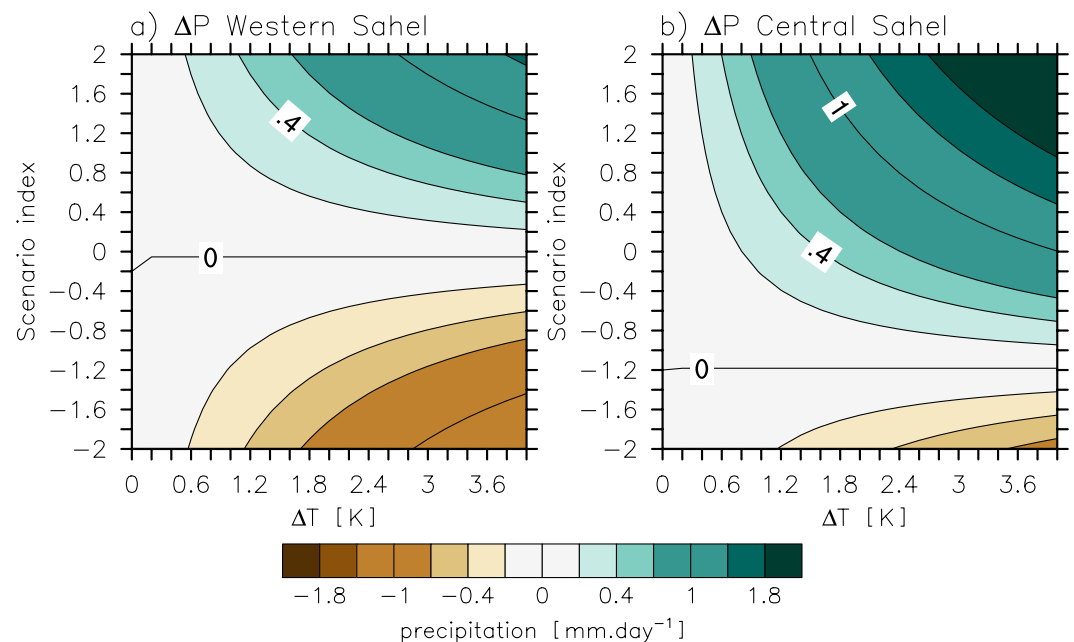


**Figure 8.** Changes in (a) western and (b) central Sahel precipitation [mm d<sup>-1</sup>], as a function of the scenario index (see text for detail) and of the magnitude of changes in global mean surface air temperature ( $\Delta T$ ).

and the result of the pattern scaling can be due to changes in the relative magnitude of the North Atlantic and Euro-Mediterranean warming in the early 21st century.

The pattern scaling approach gives similar results to the CMIP6 ensemble mean for the end of the 21st century. We then show that the A+M+ and A-M- storylines alone largely capture the spread in western and central Sahel precipitation. Therefore, the storyline approach allows simulating the breadth of the CMIP6 uncertainty in Sahel precipitation change, as defined by the ensemble spread, after the mid-21st century (Figures 7b and 7c). In other words, we further confirm that the two storylines are not outliers, as compared to the responses obtained from each CMIP6 models within the transient SSP5-8.5 emission storyline (Figures 7b and 7c).

#### 4.4. Sensitivity to the North Atlantic and Euro-Mediterranean Warming Level

The results obtained up to now have used a fixed value for the scenario index (e.g.,  $i = 1.46$  for A+M/A-M-). The values of the scenario index dictates the intensity of the change in North Atlantic and Euro-Mediterranean temperature, and can thus have strong effects on future changes in Sahel precipitation. We test the sensitivity to the scenario index by computing changes in western and central Sahel precipitation, based on  $\Delta V_x = \Delta T[a_x + i(b_x + c_x)]$ , with the scenario index ranging between -2 and +2. We computed changes in precipitation for each grid point before evaluating the western and central Sahel precipitation indices. A scenario index of +1.46 yields the same changes in precipitation as in A+M+ and a scenario index of -1.46 yields the same changes in precipitation as in A-M- (Equations 14 and 15). We focus on the two storylines that explain better the CMIP6 Sahel precipitation change uncertainty, that is A+M+ and A-M-, and we do not assess the sensitivity to the scenario index for A+M- and A-M+.

Figure 8 shows how changes in western and central Sahel precipitation are sensitive to combinations of changes in global mean surface air temperature and the scenario index. The sign of the change in western Sahel precipitation is highly sensitive to the value of the scenario index, with a negative value of  $i$  and a positive value of  $i$  leading to a decrease and an increase in precipitation, respectively (Figure 8a). The multi-model mean prediction of no change in precipitation (scenario index = 0) needs to be seen with caution since both wetting and drying are plausible depending on the amount of warming in the North Atlantic and Euro-Mediterranean regions. Over the central Sahel, the likelihood of having an increase in precipitation is high, as only with a strong negative value of  $i$  it is expected a slight decrease in precipitation (Figure 8b). Higher global-mean warming amplifies these anomalies and, in most cases, drives a larger wetting; but the uncertainty associated with the scenario index is substantial and it matches with the impact of several degrees of warming.

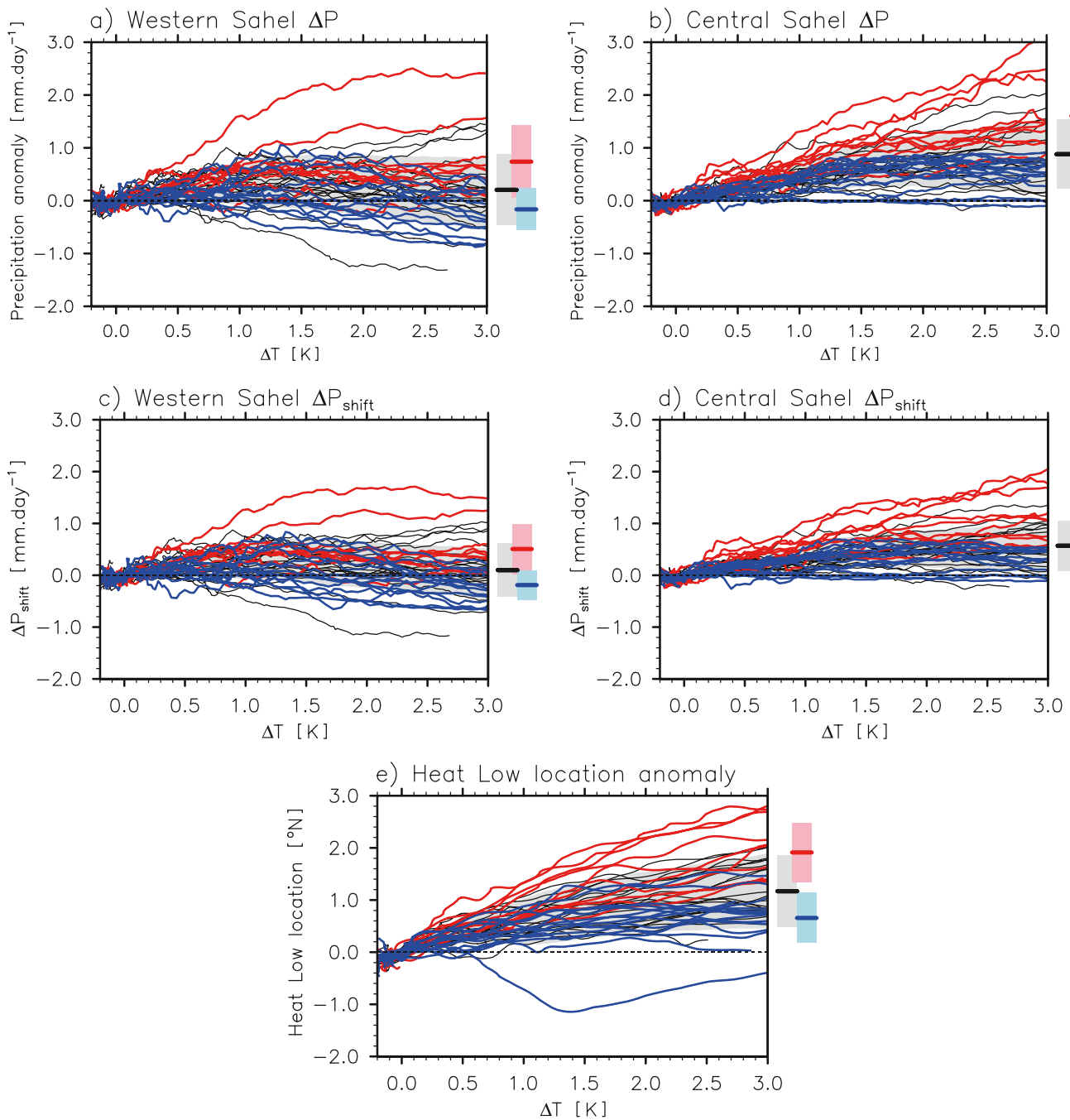


**Figure 9.** Changes in (a) western and (b) central Sahel precipitation [ $\text{mm}\cdot\text{day}^{-1}$ ] as a function of global-mean warming ( $\Delta T$ ) for all models (black lines), the CMIP6 envelope (gray shading, spanning 2 times the CMIP6 standard deviation), the A+M+ models (red), and the A-M- models (blue). (c and d) are as (a and b) but for  $\Delta P_{\text{shift}}$ . (e) Changes in the latitude of the Saharan Heat low ( $^{\circ}\text{N}$ ). On the right hand side of each panel, the horizontal thick lines indicate the ensemble mean, and the bars indicate the ensemble envelope (spanning 2 times the ensemble standard deviation), computed across the CMIP6 models (black), the A+M+ models (red) and the A-M- models (blue), for a warming of 2.5–3°C.

## 5. Mechanisms in Selected CMIP6 Models

We show the time evolution of the changes in the western (Figure 9a) and central (Figure 9b) Sahel precipitation, as a function of  $\Delta T$ , for all individual models. We then assess the effects of the A+M+ and A-M- storylines within the CMIP6 ensemble, selecting models that are showing higher and lower than average warmings of the North Atlantic and Euro-Mediterranean areas. The two new sub-ensembles are also useful to analyze mechanisms that explain changes in Sahel precipitation. We hereafter refer to as the A+M+ models, the models that lie on the

quadrants of A+M+ and that are outside of the inner ellipse (Figure 5). The A–M– models are the models that lie on the quadrants of A–M– and that are outside of the inner ellipse. We show that the A+M+ models reproduce an increase in Sahel precipitation that is stronger than the multi-model mean, while the A–M– models simulate less precipitation than the multi-model mean toward high values in  $\Delta T$  (Figures 9a and 9b).

There is a clear separation between the A+M+ and A–M– ensembles for a  $\Delta T$  of 2.5–3K, showing that both groups of models are associated with different changes in precipitation (see the bars on Figure 9). These results confirm that the rate of warming of the Euro-Mediterranean area and of the North Atlantic Ocean, relative to the global mean increase in surface air temperature, can explain a large proportion of the uncertainty in Sahel precipitation change, for high values in  $\Delta T$  (or, in other words, for the end of the 21st century).

The spread in precipitation change associated with a shift of the atmospheric circulation ( $\Delta P_{\text{shift}}$ ) is nearly identical to the one obtained for the total precipitation change, showing a strong control of the shift of the atmospheric circulation on Sahel precipitation change uncertainty (Figures 9c and 9d) within the CMIP6 ensemble, as shown in Monerie, Wainwright, et al. (2020). This is further confirmed by the A+M+ and A–M– models that show the same behavior for the change in both central and western Sahel precipitation (Figures 9a and 9b) and for  $\Delta P_{\text{shift}}$  (Figures 9c and 9d). This is also consistent with the effects of a warming of the North Atlantic SSTs, that primarily affect Sahel precipitation through dynamic changes of the circulation (Monerie et al., 2019).

We show that the change in the mean tropical circulation is less uncertain, with no strong differences between A+M+ and A–M– models in future changes in  $\Delta P_{\text{weak}}$  (Figure S3 in Supporting Information S1). The same conclusion is drawn for  $\Delta P_{\text{therm}}$  (Figure S4 in Supporting Information S1).

Uncertainty in Sahel precipitation change is therefore strongly associated with the effects of the remote drivers on the shift of the monsoon circulation. As stated in the introduction, a northward shift of the monsoon system is accompanied by a northward shift in the location of the SHL. The SHL moves northwards due to the warming of northern Africa, but the northward shift of the SHL is substantially stronger in the A+M+ models than in the A–M– models (Figure 9e).

It is surprising to see both a northward shift of the SHL and a decrease in precipitation over the western Sahel, as is the case in A–M– models. We impute the precipitation decrease in this case to the weaker warming of the North Atlantic SSTs relative to the tropical SSTs (Figure S5 in Supporting Information S1). This pattern of SST gradients leads to a southward shift of the ITCZ over the tropical Atlantic and western West Africa (Monerie et al., 2021). In addition, the warming of the tropical SSTs leads to an increase in vertical static stability over the tropics (Gaetani et al., 2017; Hill et al., 2017; Monerie et al., 2021), which directly inhibits the future increase in precipitation, and the necessary supply of moisture to meet this upped ante for convection (Chou & Neelin, 2004) cannot be provided by the nearby ocean when, as in A–M–, they are relatively cold (Giannini, 2010). This is particularly relevant here because the effect of a warming of the tropical SSTs was shown to be particularly strong over the western Sahel within the CMIP6 ensemble (Gaetani et al., 2017; Monerie, Sanchez-Gomez, et al., 2020).

## 6. Summary and Discussion

A high inter-model spread in the simulated changes in Sahel precipitation lowers our confidence in the projections. Uncertainties in Sahel precipitation were shown to derive from uncertain projections of atmospheric circulation patterns (Monerie, Wainwright, et al., 2020). In this study we use a storyline approach previously applied to extratropical circulation changes (Mindlin et al., 2020; Zappa and Shepherd, 2017) to further investigate the role of remote sources of uncertainty on the Sahel precipitation and the monsoon circulation.

We show that changes in North Atlantic and in Euro-Mediterranean temperatures explain up to 60% of the central Sahel precipitation change uncertainty. We expect some of the processes controlling the uncertainty in changes in the North Atlantic SSTs to be different to the processes controlling the uncertainty in changes in Euro-Mediterranean temperature. We then assume the selection of the two remote drivers to sample a large range of sources of climate change uncertainty. Uncertainty in future changes of the Atlantic meridional overturning circulation has strong effects on future changes in North Atlantic temperature (Bellomo et al., 2021; Swingedouw et al., 2021) while uncertainty in local land/cloud feedback rather strongly contributes to the uncertainty in surface air temperature change over Southern Europe (Boé & Terray, 2014), and thus possibly the Mediterranean Sea.

Based on these remote sources of uncertainty, we constructed four different storylines. In the A+M+ storyline, a concomitant anomalously high increase in temperature of the North Atlantic Ocean and Euro-Mediterranean area

promotes a northward shift of the Atlantic ITCZ and of the WAM, increasing precipitation in both the central and western Sahel. The dynamic shift of the monsoon system is accompanied by a northward shift of the SHL that allows strengthening low-level westerlies and increasing central Sahel precipitation. In contrast to A+M+, the A–M– storyline (small warming over both the North Atlantic and the Euro-Mediterranean temperature) is associated with a decrease in western Sahel precipitation and a smaller change in central Sahel precipitation than the multi model mean. We attribute the change in precipitation of the A–M– storyline to a cooling of the North Atlantic Ocean relative to the tropics, and to a southward shift of the ITCZ over the Atlantic Ocean and West Africa.

Interestingly, in the A+M– storyline, the effects of an anomalously large increase in North Atlantic Ocean temperature counterbalance those of an anomalously low increase in Euro-Mediterranean temperature on both the western and central Sahel precipitation, showing that both oceanic basins have a similar effect on uncertainty in Sahel precipitation change. Likewise, the A–M+ storyline also shows a cancellation of effects across the Sahel.

We acknowledge that other drivers can contribute to also help explaining changes in Sahel precipitation (Figure S6 in Supporting Information S1 and discussion in the Supporting Information S1). More specifically, a model selection can also be made based on changes in the large-scale temperature gradients (interhemispheric and northern hemisphere relative to the tropics), as suggested in Park et al. (2016) and Monerie, Wainwright, et al. (2020). However, we show that there is a large overlap between a model selection based on the A+M+ and A–M– storylines and on the large-scale temperature gradients (Figures S7, S8, and S10 in Supporting Information S1). The tropical Pacific SSTs could also be used as a driver in conjunction to the interhemispheric temperature contrast, but this explains a slightly weaker part of the uncertainty that with the drivers used here, this is discussed in the Supporting Information S1 (Figure S9).

We use the outputs of the Storyline approach to provide a method that could be helpful at selecting models for impacts studies: by selecting models based on their sensitivity to climate change over the North Atlantic and Mediterranean Sea, one can sample a large range of uncertainty in Sahel precipitation change with just few models. This method has the advantage of allowing a focus on the physical mechanisms of change in the selected models. For instance, one can address the effect of an uncertain warming of the Mediterranean Sea and the North Atlantic Ocean on future changes in precipitation extremes, dry spells, or monsoon onset, among others. This approach is therefore complementary to others that are based on patterns in precipitation change (Monerie et al., 2016) or detailed analyses of model biases (McSweeney et al., 2015).

A limitation of the study is that the storyline approach (Zappa and Shepherd, 2017) relies on a statistical analysis across the CMIP6 ensemble. We argue that a mechanistic approach should therefore also be used to assess how uncertainty in the remote drivers can lead to uncertainty in Sahel precipitation change. In future work, a first step could be achieved by prescribing SST anomalies, derived from the A+M+ and A–M– storylines, in AMIP-type simulations. In addition to anomalies in SST, experiments could include different physics of dust particles (e.g., absorption properties) and treatments of the vegetation-atmosphere feedback. This will help understanding better the mechanism by which uncertain changes in extratropical SSTs lead to uncertainty in Sahel precipitation change.

We acknowledge that in addition to changes in SSTs, uncertainty in Sahel precipitation change can also be due to (a) differences between models at simulating the amount of atmospheric mineral dust (Zhao et al., 2022) and its direct effects on the WAM system (Evan et al., 2016; Solmon et al., 2008), (b) effects of changes in vegetation cover (Wang and Alo, 2012) and land-atmosphere feedbacks (Koster et al., 2004), or (c) effects of changes in anthropogenic aerosols on Sahel precipitation (Monerie et al., 2023). (d) Differences in model's convective schemes are also strong sources of uncertainty (Ramarohetra et al., 2015; Yan et al., 2018). Moreover, feedback between changes in subtropical temperature and mineral dust amounts or vegetation cover over West Africa, through changes in wind speed, temperature, and precipitation could be a strong source of uncertainty in the Earth System Models of the CMIP6 ensemble. Further work could focus on assessing these other sources of uncertainty for Sahel precipitation change.

### Data Availability Statement

CMIP6 GCM output is available from public repositories, including <https://esgf-index1.ceda.ac.uk/search/cmip6-ceda/>.



**Acknowledgments**

We acknowledge the World Climate Research Programme, which, through its Working Group on Coupled Modelling, coordinated and promoted CMIP6. We thank the climate modeling groups for producing and making available their model output, the Earth System Grid Federation (ESGF) for archiving the data and providing access, and the multiple funding agencies who support CMIP6 and ESGF. J.M. was supported by ANR-19-JPOC-003 JPI climate/JPI ocean ROADMAP and by the ARCHANGE project of the “Make our planet great again” program (ANR-18-MPGA-0001, France). EM acknowledges the funding provided by the Spanish Ministry of Science and Competitiveness DISTRONIA (PID2021-125806NB-I00) project. G. Z. acknowledges funding from the Italian Ministry of Education, University and Research (MIUR) through the JPI Oceans/Climate ROADMAP Project (D. M. 593/2016). We thank the two anonymous reviewers for their comments and suggestions.

**References**

Baarsch, F., Granadillos, J. R., Hare, W., Knaus, M., Krapp, M., Schaeffer, M., & Lotze-Campen, H. (2020). The impact of climate change on incomes and convergence in Africa. *World Development*, 126, 104699. <https://doi.org/10.1016/j.worlddev.2019.104699>

Bellomo, K., Angeloni, M., Corti, S., & von Hardenberg, J. (2021). Future climate change shaped by inter-model differences in Atlantic meridional overturning circulation response. *Nature Communications*, 12(1), 3659. <https://doi.org/10.1038/s41467-021-24015-w>

Biasutti, M. (2013a). Forced Sahel rainfall trends in the CMIP5 archive. *Journal of Geophysical Research: Atmospheres*, 118(4), 1613–1623. <https://doi.org/10.1002/jgrd.50206>

Biasutti, M. (2013b). Forced Sahel rainfall trends in the CMIP5 archive. *Journal of Geophysical Research: Atmospheres*, 118(4), 1613–1623. <https://doi.org/10.1002/jgrd.50206>

Biasutti, M., Held, I. M., Sobel, A. H., & Giannini, A. (2008). SST forcings and Sahel rainfall variability in simulations of the twentieth and twenty-first centuries. *Journal of Climate*, 21(14), 3471–3486. <https://doi.org/10.1175/2007JCLI1896.1>

Biasutti, M., Sobel, A. H., & Camargo, S. J. (2009). The role of the Sahara low in summertime Sahel rainfall variability and change in the CMIP3 models. *Journal of Climate*, 22(21), 5755–5771. <https://doi.org/10.1175/2009JCLI2969.1>

Boé, J., & Terray, L. (2014). Land–sea contrast, soil–atmosphere and cloud–temperature interactions: Interplays and roles in future summer European climate change. *Climate Dynamics*, 42(3–4), 683–699. <https://doi.org/10.1007/s00382-013-1868-8>

Chadwick, R., Boutle, I., & Martin, G. (2013). Spatial patterns of precipitation change in CMIP5: Why the rich do not get richer in the tropics. *Journal of Climate*, 26(11), 3803–3822. <https://doi.org/10.1175/JCLI-D-12-00543.1>

Chadwick, R., Good, P., & Willett, K. (2016). A simple moisture advection model of specific humidity change over land in response to SST warming. *Journal of Climate*, 29(21), 7613–7632. <https://doi.org/10.1175/JCLI-D-16-0241.1>

Chou, C., & Neelin, J. D. (2004). Mechanisms of global warming impacts on regional tropical precipitation. *Journal of Climate*, 17(13), 2688–2701. [https://doi.org/10.1175/1520-0442\(2004\)017<2688:MOGWIO>2.0.CO;2](https://doi.org/10.1175/1520-0442(2004)017<2688:MOGWIO>2.0.CO;2)

Cissé, G. (2019). Food-borne and water-borne diseases under climate change in low- and middle-income countries: Further efforts needed for reducing environmental health exposure risks. *Acta Tropica*, 194, 181–188. <https://doi.org/10.1016/j.actatropica.2019.03.012>

Dixon, R. D., Daloz, A. S., Vimont, D. J., & Biasutti, M. (2017). Saharan heat low biases in CMIP5 models. *Journal of Climate*, 30(8), 2867–2884. <https://doi.org/10.1175/JCLI-D-16-0134.1>

Dixon, R. D., Vimont, D. J., & Daloz, A. S. (2018). The relationship between tropical precipitation biases and the Saharan heat low bias in CMIP5 models. *Climate Dynamics*, 50(9–10), 3729–3744. <https://doi.org/10.1007/s00382-017-3838-z>

Dong, B., & Sutton, R. (2015). Dominant role of greenhouse-gas forcing in the recovery of Sahel rainfall. *Nature Climate Change*, 5(8), 757–760. <https://doi.org/10.1038/nclimate2664>

Evan, A. T., Flamant, C., Gaetani, M., & Guichard, F. (2016). The past, present and future of African dust. *Nature*, 531(7595), 493–495. <https://doi.org/10.1038/nature17149>

Eyring, V., Bony, S., Meehl, G. A., Senior, C. A., Stevens, B., Stouffer, R. J., & Taylor, K. E. (2016). Overview of the Coupled Model Inter-comparison Project Phase 6 (CMIP6) experimental design and organization. *Geoscientific Model Development*, 9(5), 1937–1958. <https://doi.org/10.5194/gmd-9-1937-2016>

Fontaine, B., Garcia-Serrano, J., Roucou, P., Rodriguez-Fonseca, B., Losada, T., Chauvin, F., et al. (2010). Impacts of warm and cold situations in the Mediterranean basins on the West African monsoon: Observed connection patterns (1979–2006) and climate simulations. *Climate Dynamics*, 35(1), 95–114. <https://doi.org/10.1007/s00382-009-0599-3>

Gaetani, M., Flamant, C., Bastin, S., Janicot, S., Lavaysse, C., Hourdin, F., et al. (2017). West African monsoon dynamics and precipitation: The competition between global SST warming and CO<sub>2</sub> increase in CMIP5 idealized simulations. *Climate Dynamics*, 48(3–4), 1353–1373. <https://doi.org/10.1007/s00382-016-3146-z>

Giannini, A. (2010). Mechanisms of climate change in the semiarid African Sahel: The local view. *Journal of Climate*, 23(3), 743–756. <https://doi.org/10.1175/2009JCLI3123.1>

Giannini, A., Salack, S., Lodoun, T., Ali, A., Gaye, A. T., & Ndiaye, O. (2013). A unifying view of climate change in the Sahel linking intra-seasonal, interannual and longer time scales. *Environmental Research Letters*, 8(2), 24010. <https://doi.org/10.1088/1748-9326/8/2/024010>

Held, I. M., & Soden, B. J. (2006). Robust responses of the hydrological cycle to global warming. *Journal of Climate*, 19(21), 5686–5699. <https://doi.org/10.1175/JCLI3990.1>

Herman, R. J., Giannini, A., Biasutti, M., & Kushnir, Y. (2020). The effects of anthropogenic and volcanic aerosols and greenhouse gases on twentieth century Sahel precipitation. *Scientific Reports*, 10(1), 12203. <https://doi.org/10.1038/s41598-020-68356-w>

Hill, S. A., Ming, Y., Held, I. M., & Zhao, M. (2017). A moist static energy budget–based analysis of the Sahel rainfall response to uniform oceanic warming. *Journal of Climate*, 30(15), 5637–5660. <https://doi.org/10.1175/JCLI-D-16-0785.1>

Hirasawa, H., Kushner, P. J., Sigmond, M., Fyfe, J., & Deser, C. (2020). Anthropogenic aerosols dominate forced multidecadal Sahel precipitation change through distinct atmospheric and oceanic drivers. *Journal of Climate*, 1–56(23), 10187–10204. <https://doi.org/10.1175/JCLI-D-19-0829.1>

Jankowska, M. M., Lopez-Carr, D., Funk, C., Husak, G. J., & Chafe, Z. A. (2012). Climate change and human health: Spatial modeling of water availability, malnutrition, and livelihoods in Mali, Africa. *Applied Geography*, 33, 4–15. <https://doi.org/10.1016/j.apgeog.2011.08.009>

Koster, R. D., Dirmeyer, P. A., Guo, Z., Bonan, G., Chan, E., Cox, P., et al. (2004). Regions of strong coupling between soil moisture and precipitation. *Science*, 305(5687), 1138–1140. <https://doi.org/10.1126/science.1100217>

Lavaysse, C., Flamant, C., Evan, A., Janicot, S., & Gaetani, M. (2016). Recent climatological trend of the Saharan heat low and its impact on the West African climate. *Climate Dynamics*, 47(11), 3479–3498. <https://doi.org/10.1007/s00382-015-2847-z>

Lavaysse, C., Flamant, C., Janicot, S., Parker, D. J., Lafore, J. P., Sultan, B., & Pelon, J. (2009). Seasonal evolution of the West African heat low: A climatological perspective. *Climate Dynamics*, 33(2–3), 313–330. <https://doi.org/10.1007/s00382-009-0553-4>

Liu, Y., Chiang, J. C. H., Chou, C., & Patricola, C. M. (2014). Atmospheric teleconnection mechanisms of extratropical North Atlantic SST influence on Sahel rainfall. *Climate Dynamics*, 43(9–10), 2797–2811. <https://doi.org/10.1007/s00382-014-2094-8>

Manzini, E., Karpechko, A. Y., Anstey, J., Baldwin, M. P., Black, R. X., Cagnazzo, C., et al. (2014). Northern winter climate change: Assessment of uncertainty in CMIP5 projections related to stratosphere-troposphere coupling. *Journal of Geophysical Research: Atmospheres*, 119(13), 7979–7998. <https://doi.org/10.1002/2013JD021403>

Marega, O., Mering, C., & Meunier, V. (2018). Sahelian agro-pastoralists in the face of social and environmental changes: New issues, new risks, new transhumance axe. *LEspace Géographique*, 47(3), 235–260. <https://doi.org/10.3917/eg.473.0235>

Martin, E. R., & Thorncroft, C. D. (2014). The impact of the AMO on the West African monsoon annual cycle. *Quarterly Journal of the Royal Meteorological Society*, 140(678), 31–46. <https://doi.org/10.1002/qj.2107>

- Marvel, K., Biasutti, M., & Bonfils, C. (2020). Fingerprints of external forcing agents on Sahel rainfall: Aerosols, greenhouse gases, and model-observation discrepancies. *Environmental Research Letters*, *15*(8), 084023. <https://doi.org/10.1088/1748-9326/ab858e>
- McSweeney, C. F., Jones, R. G., Lee, R. W., & Rowell, D. P. (2015). Selecting CMIP5 GCMs for downscaling over multiple regions. *Climate Dynamics*, *44*(11–12), 3237–3260. <https://doi.org/10.1007/s00382-014-2418-8>
- Mindlin, J., Shepherd, T. G., Vera, C. S., Osman, M., Zappa, G., Lee, R. W., & Hodges, K. I. (2020). Storyline description of Southern Hemisphere midlatitude circulation and precipitation response to greenhouse gas forcing. *Climate Dynamics*, *54*(9–10), 4399–4421. <https://doi.org/10.1007/s00382-020-05234-1>
- Mohino, E., Janicot, S., & Bader, J. (2011). Sahel rainfall and decadal to multi-decadal sea surface temperature variability. *Climate Dynamics*, *37*(3–4), 419–440. <https://doi.org/10.1007/s00382-010-0867-2>
- Monerie, P.-A., Dittus, A. J., Wilcox, L. J., & Turner, A. G. (2023). Uncertainty in simulating twentieth century West African precipitation trends: The role of anthropogenic aerosol emissions. *Earth's Future*, *11*(2), e2022EF002995. <https://doi.org/10.1029/2022EF002995>
- Monerie, P.-A., Pohl, B., & Gaetani, M. (2021). The fast response of Sahel precipitation to climate change allows effective mitigation action. *Npj Climate and Atmospheric Science*, *4*(1), 24. <https://doi.org/10.1038/s41612-021-00179-6>
- Monerie, P.-A., Robson, J., Dong, B., Hodson, D. L. R., & Klingaman, N. P. (2019). Effect of the Atlantic multidecadal variability on the global monsoon. *Geophysical Research Letters*, *46*(3), 1765–1775. <https://doi.org/10.1029/2018GL080903>
- Monerie, P.-A., Sanchez-Gomez, E., & Boé, J. (2016). On the range of future Sahel precipitation projections and the selection of a sub-sample of CMIP5 models for impact studies. *Climate Dynamics*, *48*(7–8), 2751–2770. <https://doi.org/10.1007/s00382-016-3236-y>
- Monerie, P.-A., Sanchez-Gomez, E., Gaetani, M., Mohino, E., & Dong, B. (2020). Future evolution of the Sahel precipitation zonal contrast in CESM1. *Climate Dynamics*, *55*(9–10), 2801–2821. <https://doi.org/10.1007/s00382-020-05417-w>
- Monerie, P.-A., Wainwright, C. M., Sidibe, M., & Akinsanola, A. A. (2020). Model uncertainties in climate change impacts on Sahel precipitation in ensembles of CMIP5 and CMIP6 simulations. *Climate Dynamics*, *55*(5–6), 1385–1401. <https://doi.org/10.1007/s00382-020-05332-0>
- Monerie, P.-A., Wilcox, L. J., & Turner, A. G. (2022). Effects of anthropogenic aerosol and greenhouse gas emissions on Northern Hemisphere monsoon precipitation: Mechanisms and uncertainty. *Journal of Climate*, *1–66*(8), 2305–2326. <https://doi.org/10.1175/JCLI-D-21-0412.1>
- Mutton, H., Chadwick, R., Collins, M., Lambert, F. H., Geen, R., Todd, A., & Taylor, C. M. (2022). The impact of the direct radiative effect of increased CO<sub>2</sub> on the West African Monsoon. *Journal of Climate*, *35*(8), 2441–2458. <https://doi.org/10.1175/JCLI-D-21-0340.1>
- Ndiaye, C. D., Mohino, E., Mignot, J., & Sall, S. M. (2022). On the detection of externally-forced decadal modulations of the Sahel rainfall over the whole 20th century in the CMIP6 ensemble. *Journal of Climate*, *1–51*(21), 6939–6954. <https://doi.org/10.1175/JCLI-D-21-0585.1>
- O'Neill, B. C., Tebaldi, C., van Vuuren, D. P., Eyring, V., Friedlingstein, P., Hurtt, G., et al. (2016). The Scenario Model Intercomparison Project (ScenarioMIP) for CMIP6. *Geoscientific Model Development*, *9*, 3461–3482. <https://doi.org/10.5194/gmd-9-3461-2016>
- Park, J., Bader, J., & Matei, D. (2016). Anthropogenic Mediterranean warming essential driver for present and future Sahel rainfall. *Nature Climate Change*, *6*(10), 941–945. <https://doi.org/10.1038/nclimate3065>
- Park, J.-Y., Bader, J., & Matei, D. (2015). Northern-hemispheric differential warming is the key to understanding the discrepancies in the projected Sahel rainfall. *Nature Communications*, *6*(1), 5985. <https://doi.org/10.1038/ncomms6985>
- Ramarohetra, J., Pohl, B., & Sultan, B. (2015). Errors and uncertainties introduced by a regional climate model in climate impact assessments: Example of crop yield simulations in West Africa. *Environmental Research Letters*, *10*(12), 124014. <https://doi.org/10.1088/1748-9326/10/12/124014>
- Ramin, B. M., & McMichael, A. J. (2009). Climate change and health in sub-Saharan Africa: A case-based perspective. *EcoHealth*, *6*(1), 52–57. <https://doi.org/10.1007/s10393-009-0222-4>
- Roehrig, R., Chauvin, F., & Lafore, J.-P. (2011). 10–25-day intraseasonal variability of convection over the Sahel: A role of the Saharan heat low and midlatitudes. *Journal of Climate*, *24*(22), 5863–5878. <https://doi.org/10.1175/2011JCLI3960.1>
- Rowell, D. P. (2003). The impact of Mediterranean SSTs on the Sahelian rainfall Season. *Journal of Climate*, *16*(5), 849–862. [https://doi.org/10.1175/1520-0442\(2003\)016<0849:TIOMSO>2.0.CO;2](https://doi.org/10.1175/1520-0442(2003)016<0849:TIOMSO>2.0.CO;2)
- Sainte Fare Garnot, V., Groth, A., & Ghil, M. (2018). Coupled climate-economic modes in the Sahel's interannual variability. *Ecological Economics*, *153*, 111–123. <https://doi.org/10.1016/j.ecolecon.2018.07.006>
- Sanogo, S., Fink, A. H., Omotosho, J. A., Ba, A., Redl, R., & Ermert, V. (2015). Spatio-temporal characteristics of the recent rainfall recovery in West Africa. *International Journal of Climatology*, *35*(15), 4589–4605. <https://doi.org/10.1002/joc.4309>
- Schneider, T., Bischoff, T., & Haug, G. H. (2014). Migrations and dynamics of the intertropical convergence zone. *Nature*, *513*(7516), 45–53. <https://doi.org/10.1038/nature13636>
- Shekhar, R., & Boos, W. R. (2017). Weakening and shifting of the Saharan shallow meridional circulation during wet years of the West African Monsoon. *Journal of Climate*, *30*(18), 7399–7422. <https://doi.org/10.1175/JCLI-D-16-0696.1>
- Solmon, F., Mallet, M., Elguindi, N., Giorgi, F., Zakey, A., & Konaré, A. (2008). Dust aerosol impact on regional precipitation over western Africa, mechanisms and sensitivity to absorption properties. *Geophysical Research Letters*, *35*(24), L24705. <https://doi.org/10.1029/2008GL035900>
- Sultan, B., & Gaetani, M. (2016). Agriculture in West Africa in the twenty-first century: Climate change and impacts scenarios, and potential for adaptation. *Frontiers of Plant Science*, *7*, 1262. <https://doi.org/10.3389/fpls.2016.01262>
- Swingedouw, D., Bily, A., Esquerdo, C., Borchert, L. F., Sgubin, G., Mignot, J., & Menary, M. (2021). On the risk of abrupt changes in the North Atlantic subpolar gyre in CMIP6 models. *Annals of the New York Academy of Sciences*, *1504*(1), 187–201. <https://doi.org/10.1111/nyas.14659>
- Taylor, K. E., Stouffer, R. J., & Meehl, G. A. (2012). An overview of CMIP5 and the experiment design. *Bulletin American Meteorology Soc.*, *93*(4), 485–498. <https://doi.org/10.1175/bams-d-11-00094.1>
- Tebaldi, C., & Arblaster, J. M. (2014). Pattern scaling: Its strengths and limitations, and an update on the latest model simulations. *Climate Change*, *122*(3), 459–471. <https://doi.org/10.1007/s10584-013-1032-9>
- Wang, G., & Alo, C. A. (2012). Changes in precipitation seasonality in West Africa predicted by RegCM3 and the impact of dynamic vegetation feedback. *International Journal of Geophysics*, *2012*, 1–10. <https://doi.org/10.1155/2012/597205>
- Yan, Y., Lu, R., & Li, C. (2018). Relationship between the future projections of Sahel rainfall and the simulation biases of present South Asian and Western North Pacific rainfall in summer. *Journal of Climate*, *32*(4), 1327–1343. <https://doi.org/10.1175/JCLI-D-17-0846.1>
- Zappa, G., & Shepherd, T. G. (2017). Storylines of atmospheric circulation change for European regional climate impact assessment. *Journal of Climate*, *30*(16), 6561–6577. <https://doi.org/10.1175/JCLI-D-16-0807.1>
- Zhao, A., Ryder, C. L., & Wilcox, L. J. (2022). How well do the CMIP6 models simulate dust aerosols? *Atmospheric Chemistry and Physics*, *22*(3), 2095–2119. <https://doi.org/10.5194/acp-22-2095-2022>